Groundwater quality and associated hydrogeochemical processes in Northwest Namibia

Article *in* Journal of Geochemical Exploration · December 2017

DOI: 10.1016/j.gexplo.2017.12.015

8 authors, including:

Li Zhihong
China University of Geosciences (Beijing)
3 PUBLICATIONS **12** CITATIONS
SEE PROFILE

Guangcai Wang
China University of Geosciences (Beijing)
96 PUBLICATIONS **567** CITATIONS
SEE PROFILE

Zheming Shi
China University of Geosciences (Beijing)
40 PUBLICATIONS **242** CITATIONS
SEE PROFILE

Heike Wanke
University of the West of England, Bristol
37 PUBLICATIONS **190** CITATIONS
SEE PROFILE

Journal of Geochemical Exploration 186 (2018) 202–214

Contents lists available at ScienceDirect

Journal of Geochemical Exploration

journal homepage: www.elsevier.com/locate/gexplo

Groundwater quality and associated hydrogeochemical processes in Northwest Namibia

Zhihong Li[a,e], Guangcai Wang[a,b,*], Xusheng Wang[b,c], Li Wan[b], Zheming Shi[b,c], Heike Wanke[d,**], Shoopala Uugulu[d], Collen-Issia Uahengo[d]

[a] State Key Laboratory of Biogeology and Environmental Geology, China University of Geosciences, Beijing 100083, China
[b] School of Water Resources and Environment, China University of Geosciences, Beijing 100083, China
[c] MOE Key Laboratory of Groundwater Circulation and Environment Evolution, China University of Geosciences, Beijing 100083, China
[d] Department of Geology, University of Namibia, Windhoek, Namibia
[e] Center for Hydrogeology and Environmental Geology Survey, China Geological Survey, Baoding 071051, Hebei, China

ARTICLE INFO

Keywords:
Groundwater quality
Salinization
Hydrogeochemical processes
Multivariate statistics
Water-rock interaction
Northwest Namibia

ABSTRACT

Namibia is one of the driest countries in southern Africa. Groundwater has played an important role in the development of Namibia. However, like those at some other places in Namibia, groundwater is unsuitable for drinking in parts of the Northwest of Namibia because of its poor quality. It is significant to assess groundwater quality and understand the hydrogeochemical processes for the management and utilization of groundwater resource in this water-short region. In this paper, we report the investigation and assessment of groundwater quality and associated hydrogeochemical processes in the Cuvelai-Etosha Basin and Kaokoveld region, northwestern Namibia. A total of 24 samples were collected for chemistry and stable hydrogen and oxygen isotopes analysis. The groundwater quality was evaluated by single factor index method. Hydrochemical and isotopic (δD and $\delta^{18}O$) data were used to study the hydrogeochemical processes of groundwater in the areas. The results show that most of the groundwater that originated from precipitation was unacceptable in appearance and tastes, but may be safe for human consumption. The salinity and concentrations of As, U and F^- in some of groundwater samples exceeded of the WHO standards. The salinity increase of the groundwater is primarily due to minerals dissolution rather than evaporation. A number of the samples located in the Cuvelai-Etosha Basin and Kaokoveld region are low in TDS. The salinity of them mainly derives from the dissolution of carbonate. Some of the samples located in the west of the Cuvelai-Etosha Basin and Kaokoveld region have medium TDS. The salinity of them originates mainly from the dissolution of carbonate and the oxidation of pyrite. The highest Fe concentration in these samples is up to 13 mg/L. The samples located to the east of Etosha Pan have high TDS. Halite and carbonate dissolution with strong cation exchange are the major source of the high salinity. The low Ca^{2+} concentrations in groundwater and rich fluorine sediments in Cuvelai-Etosha Basin favor the formation of high F^- groundwater. The weak alkaline environment and high HCO_3^- contents are significant to the higher As and U contents. Insight from this study may be helpful to enhance the understanding of distributions and transfers of major ions and trace elements in groundwater and to improve the management and utilization of groundwater resources in the region and other similar areas.

1. Introduction

Groundwater has played a significant role in Namibia, one of the driest countries in southern Africa. Rainfall events constantly change and are unevenly distributed in space and time in Namibia (Bao et al., 1998). In addition, the high temperature in the rainy season and huge evaporation losses make Namibia the driest country in southern Africa (Christelis and Struckmeier, 2001), and groundwater is the major source of drinking water.

However, in many areas of Namibia, groundwater as a source of water supply is constrained by the limited water availability, little and unreliable recharge, low borehole yield, great depths, poor quality and high risks of contamination. Even in the region rich in groundwater, it might still be unsuitable for human consumption because of its poor quality, such as that in the Cuvelai-Etosha Basin, which is a densely populated region in Namibia. This region is characterized by seasonal

* Correspondence to: G. Wang, School of Water Resources and Environment, China University of Geosciences, Beijing 100083, China.
** Corresponding author.
E-mail addresses: wanggc@pku.edu.cn (G. Wang), hwanke@unam.na (H. Wanke).

https://doi.org/10.1016/j.gexplo.2017.12.015
Received 19 September 2016; Received in revised form 7 October 2017; Accepted 18 December 2017
Available online 20 December 2017

alterations of droughts and heavy rainfall, and often saline groundwater (Kluge et al., 2008; Lindenmaier et al., 2014). Groundwater plays a considerable role for water supply in Cuvelai-Etosha Basin, even though the quality of groundwater over much of the basin is extremely poor. Kaokoveld region generally has a low groundwater potential. However, the entire area is dependent on groundwater resources for domestic purposes and livestock watering (Christelis and Struckmeier, 2001).

Few studies have been done in the effort of understanding the groundwater quality and hydrochemical evolution in the Northwest of Namibia. The previous works dealt with the study on a few thermal springs in the entire Namibia, and preliminary investigations on the salinity or utilization of groundwater. No systematic study has been done on the groundwater quality and the hydrochemical evolution in the Northwest of Namibia. Sracek et al. (2015) explained the geochemical and isotopic composition of six geothermal springs of Namibia and showed that all of them have higher fluoride and SO_4^{2-} concentrations than both the WHO limit and the Namibian guideline, and are not suitable for drinking. Wanke et al. (2014) assessed the water quality in four regions in Namibia only for shallow aquifers that are accessed by hand dug wells. The book, "Groundwater in Namibia" (Christelis and Struckmeier, 2001) introduced the overall quality of groundwater in Cuvelai-Etosha Basin and Kaokoveld region and suggested that the quality of groundwater is extremely poor. To ensure successful groundwater exploitation (quality and quantity), it is necessary to study in detail the quality of groundwater in the area (Chukwura et al., 2015). Understanding of the quality and hydrochemical evolution of the groundwater is significant for the management and utilization of groundwater resource in the Cuvelai-Etosha Basin and Kaokoveld region.

The methods assessing the groundwater quality includes single factor index method, Nemero index method, principal component analysis method, and fuzzy comprehensive evaluation method (Yan et al., 2015; Feng and Zhang, 2012; Zhang et al., 2014; Chukwura et al., 2015; Yang and Yang, 2015). Among them, single factor index is calculated by comparing the measured value with the standard value of evaluation. This is a brief and direct, but strict method. The groundwater is thought to be unfit for human consumption when only one index exceeds the standard. In the contexts of groundwater compositions, Gibbs (1970) proposed the major natural mechanisms controlling world water chemistry, which can be classified as atmospheric precipitation, rock weathering dominance and the evaporation-crystallization processes. The common methods to analyze the chemical data are graphical and statistical methodologies (Güler et al., 2002; Chukwura et al., 2015; Yidana and Yidana, 2010; Yidana et al., 2010). Stable oxygen and hydrogen isotopes are good indicators of groundwater recharge processes and evaporation (Wang et al., 2013; Qian et al., 2013; Qian et al., 2014). Deuterium excess is a potential tool for determining the water salinization mechanism (Huang and Pang, 2012). Ion relation scatter diagram is an available method to analyze the water-rock interactions (Wang, 1990).

In this study, single factor index method comparing the major and trace elements concentrations with water quality standards are used to evaluate the groundwater quality. Graphical methods and multivariate statistical methods are used to analyze the hydrochemistry and isotope data to reveal the sources of the salinity and trace elements of the groundwater in the study area.

2. Study area

2.1. Location, climate and hydrology

The study area is located in the Northwest of Namibia and extends from 13.09° to 17.28° E and from 17.58° to 19.92° S (Fig. 1). The area consists of the Cuvelai-Etosha Basin (watershed 1 in Fig. 2), and Kaokoveld region in the west.

Most of the study area belongs to the subtropical semi-arid climate zone. The average annual rainfall ranges from 50 mm/a in the southwest to 500 mm/a in the northeast of the study area. The average annual temperatures range from 18 °C to 22 °C. Except for Kunene River, the boundary river of Namibia and Angola, there is no perennial rivers in the study area. Topographic gradients are extremely low within the Cuvelai-Etosha Basin and all drainage systems converge towards a common low point, the Etosha Pan. Floods occasionally reach the Etosha Pan when there are exceptionally heavy rains in the Angolan highlands or the Namibian part of the basin (Lindenmaier et al., 2014). Based on the elevation data downloaded from the website of CGIAR Consortium for Spatial Information, the watersheds were distinguished by the hydrological analysis method of ARCGIS (Fig. 2).

2.2. Geology and hydrogeology

The lithological units of the study area, simplified and modified after Schwartz (2006), are displayed in Fig. 3. The lithological units from oldest to youngest are as follows:

(1) Shale, siltstone, low-carbonate metamorphic rocks and igneous rocks (470–2600 Ma)
(2) Sandstone, conglomerate and volcanic rocks (132–300 Ma)
(3) Dolomite, limestone and marble
(4) Sands with subordinate calcrete
(5) Sand

The geological log of the East Kaokobelt in the northwest of the study area is displayed in Fig. 4a (Shan et al., 2012).

The Etosha Pan has the highest abundance of clays in the underlying Kalahari succession and supposedly represents the area covered by a former and much larger Paleo-lake Etosha (Lindenmaier et al., 2014). The lithological units observed in a borehole to the east of Etosha Pan through the Clay Member are shown in Fig. 4b. Under 1 m sand soil, there is 5 m of the calcrete. There is 1 m of limestone underlying the calcrete. The limestone is, in turn, underlain by two sections of clay of the Etosha Pan Clay Member, respectively 9 m and 12 m thick, separated by 36 m of a highly permeable, pale green, clayey sand aquifer patchily cemented by nodules of calcrete and dolocrete (Miller et al., 2010).

Up to now, only a small part of the hydrogeological potential of Cuvelai-Etosha Basin has been explored (Lindenmaier et al., 2014). In the centre around Oshivelo of Cuvelai-Etosha Basin, the aquifers are subdivided into the Unconfined Kalahari Aquifer (UKA_{AN}) and the Oshivelo Artesian Aquifer (OAA). The UKA_{AN} covers most of the Oshivelo and extends to the Omuramba Akazulu on the north and northeast towards the Okavango River. The water quality deteriorates within a short distance from fresh to brackish. The OAA was first penetrated at Oshivelo where it was separated by a 13 m clay layer from the overlying UKA_{AN}. The piezometric head of the OAA groundwater is higher than the surface elevation. The salinity of the artesian groundwater ranges from 600 to 1500 mg/L, deteriorating towards the north-west where TDS exceed 2600 mg/L. In the south and west of the Cuvelai-Etosha Basin, the aquifer is the Unconfined Kalahari Aquifer (UKA_{EL}). The UKA_{EL} consists of calcrete and limestone classified as fractured aquifer. The groundwater of the fractured aquifer flows into the UKA_{AN}, and eventually discharges into the Etosha Pan. The groundwater is fresh, but is vulnerable to pollution resulting locally high nitrate concentration (Christelis and Struckmeier, 2001).

Over all, all the groundwater within the Cuvelai-Etosha basin flows towards the Etosha Pan. The water quality is especially poor in the central Cuvelai-Etosal Basin with maximum TDS over 5000 mg/L. North of the Etosha Pan, the Kalahari and Karoo sequence and the upper part of the Owamboo Formation formed a large reservoir containing highly saline groundwater with TDS ranging from 30,000 to 100,000 mg/L (Christelis and Struckmeier, 2001). From Etosha Pan towards west and south, the groundwater quality improves, and the

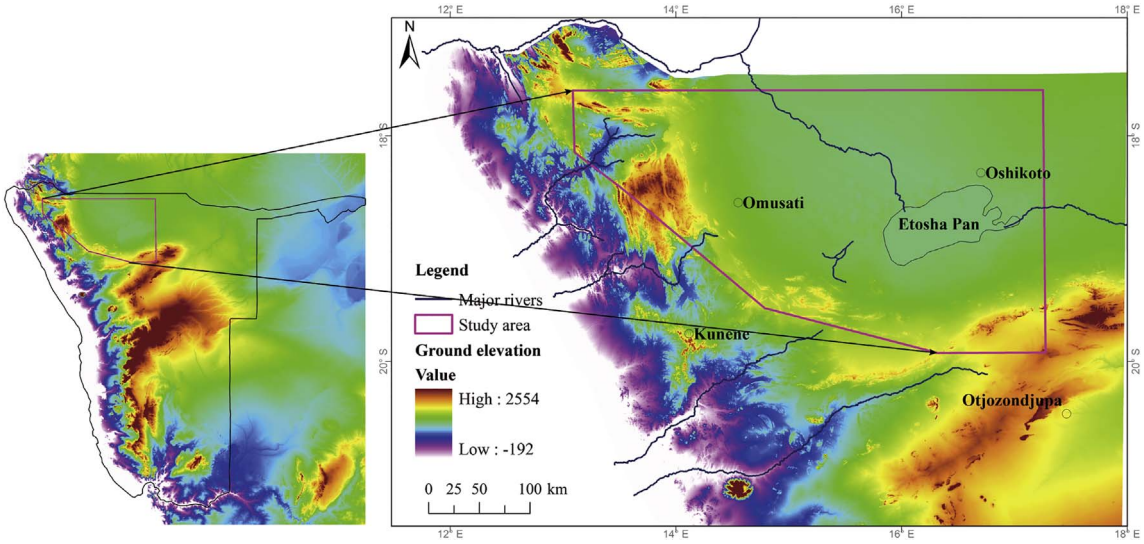

Fig. 1. Location and topography of the study area.

TDS of the groundwater can be < 1000 mg/L (Kluge et al., 2008).

In the Kaokoveld region, the groundwater is mainly stored in the fractured zones and faults, so the aquifer is classified as fractured aquifer. This region generally has a low groundwater potential decreasing westwards. Owing to the lack of surface water, the entire area is dependent on groundwater resources for domestic purposes and stock watering. It is well known that a few springs provide water for wildlife and villages and thermal springs for wildlife in Kaokoveld region (Christelis and Struckmeier, 2001). The groundwater quality may deteriorate due to over-abstraction and/or high concentrations of iron in the Chuos Formation with iron ore.

3. Sampling and methods

A sampling campaign was conducted in the area in December 2014. The distribution of samples shows in Fig. 2. The quality and hydrochemical characteristics of groundwater mainly depend on the chemical composition of the rocks that the water comes into contact with and the effect of human activities. Generally, the closer the space distance is, the more similar the chemical composition of the rocks and the effect of human activities are, and then the more similar the quality and hydrochemical characteristics of groundwater are. In order to study the quality and hydrochemical characteristics of groundwater in different subareas, the samples were divided into five groups (Fig. 2) based on the surface watersheds as insufficient information on the groundwater systems is available. Group A contains NW10 and NW11; Group B

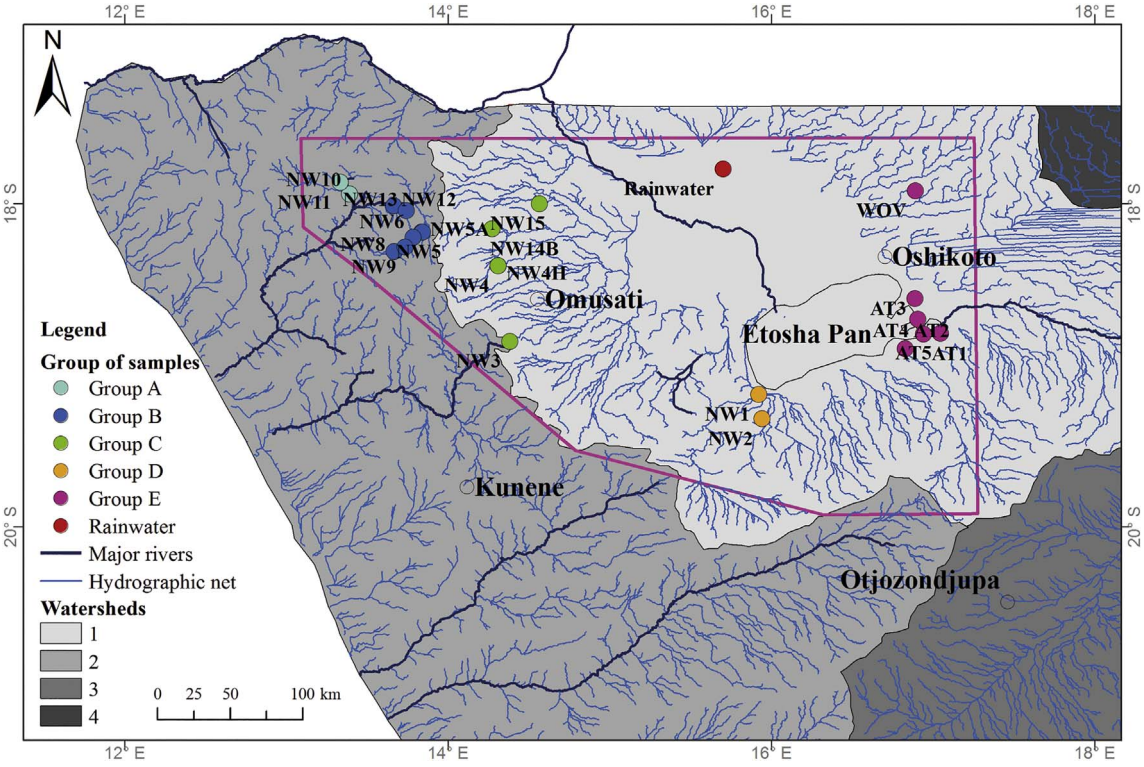

Fig. 2. Watersheds and distribution of water samples in the study area.

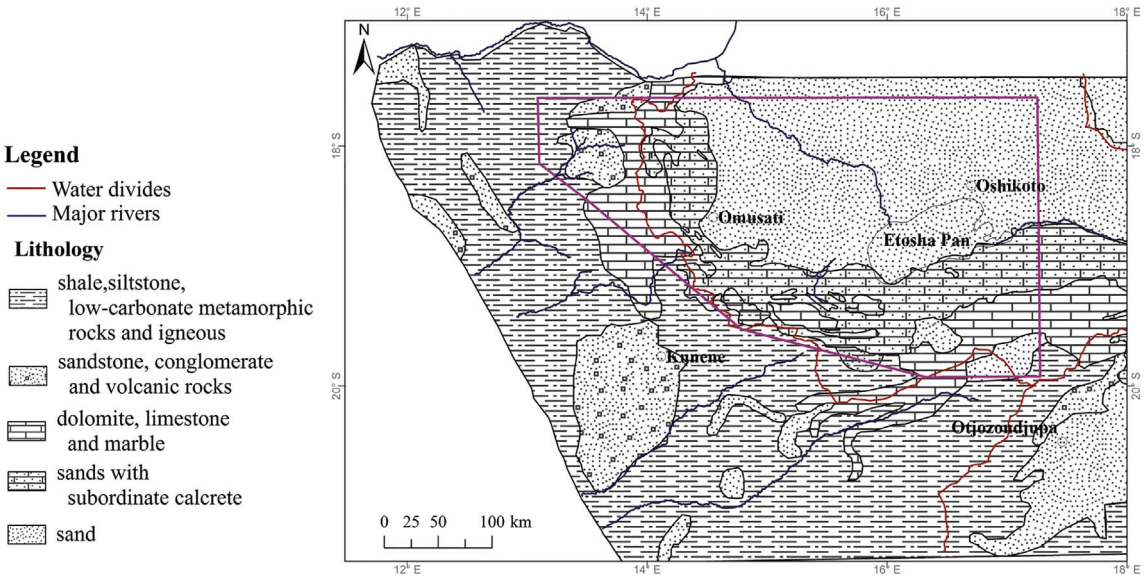

Fig. 3. Sketch lithological map of the study area (after Schwartz, 2006).

contains NW5, NW5A, NW6, NW8, NW9, NW12, and NW13; Group C contains NW3, NW4, NW4H, NW14B, and NW15; Group D contains NW1 and NW2, and Group E contains AT1, AT2, AT3, AT4, AT5, and WOV. The samples NW6, NW8, NW11, AT2, and AT3 were collected from springs. NW3, NW5A, NW12, NW14B, and NW15 were collected from boreholes with the depth of 10–50 m. NW1, NW2, NW4, NW9, AT1, and AT5 were collected from boreholes with the depth of 50–100 m. AT4, NW13, and WOV were collected from boreholes with the depth of 50–150 m. NW4H was collected from a tank stored the pumped water from the borehole of NW4. NW5 was collected from a tank stored the pumped water from the borehole of NW5A. NW10 was collected from a closed water-hole with depth of 5.3 m near a dried river.

Water samples were collected and filtered through 0.45 μm membranes into high-density polypropylene (HDPP) bottles. Electrical conductivity (EC), Oxidation-Reduction Potential (ORP) and pH were

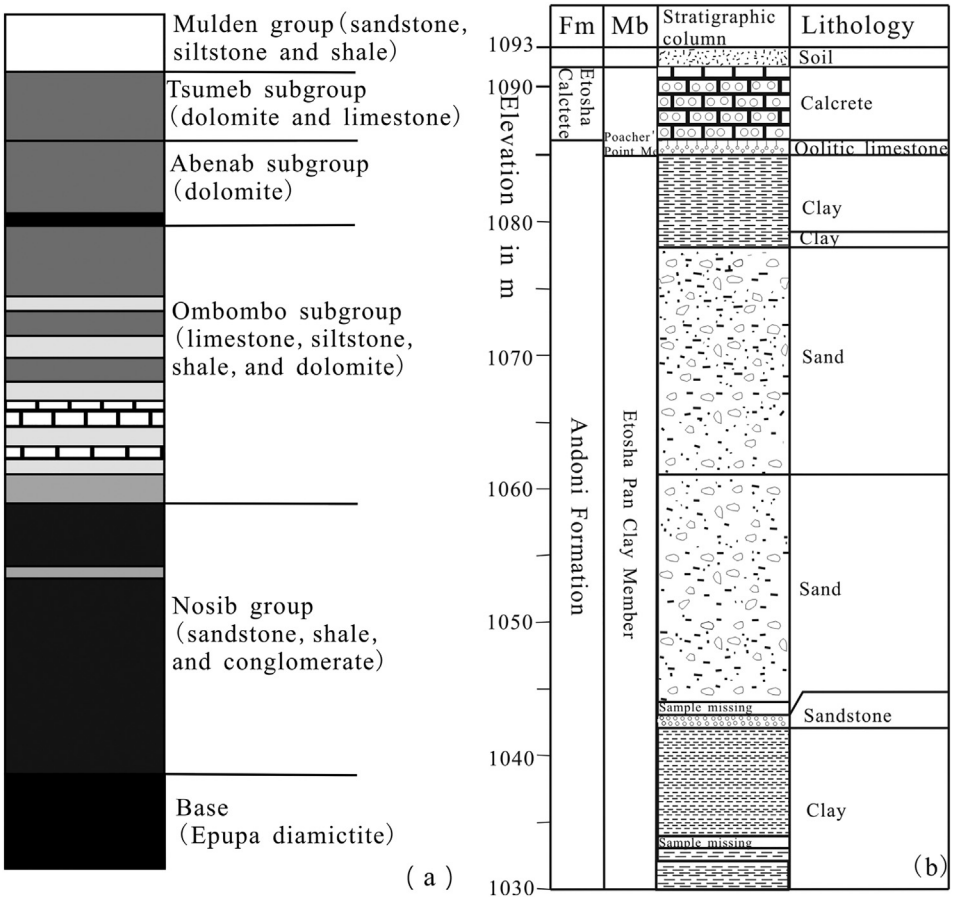

Fig. 4. Geological log of the East Kaoko belt (a) and the Owambo Basin (b). ((a) Shan et al., 2012, (b) Miller et al., 2010).

measured in situ using portable instrument (HACH) calibrated before use. The ions (K^+, Na^+, Ca^{2+}, Mg^{2+}, Cl^-, SO_4^{2-}, NO_3^-, NO_2^-, Br^-, F^-), Alkalinity as $CaCO_3$, Fe, Mn, U, As and turbidity were analyzed at the Analytical Laboratory Services Company of Windhoek, Namibia. This company regularly takes part in Proficiency Testing Schemes, and the assessment results are acceptable. During the test of water samples, quality control samples were analyzed to monitor accuracy. Samples for As analysis were acidified with ultra-pure H_2SO_4 to pH < 2. Samples for U analysis were acidified with ultra-pure HNO_3 to the nitric acid concentration of 1 mol/L. Samples for NO_3^- and NO_2^- were acidified with ultra-pure H_2SO_4 to pH < 2 with cold storage. The concentrations of cations, Fe, Mn, U and As were analyzed by inductively coupled plasma optical omission spectrometry (ICP-OES) generating data with detection limit of 0.01 mg/L for Fe, Mn, U and As, and of 0.1 mg/L for the other cations. Alkalinity was determined using titrimetric method. NO_3^- and NO_2^- were analyzed by colorimetric method. Turbidity, SO_4^{2-}, F^-, Cl^-, and Br^- were measured using nephelometric, turbidimetric, electrometric, potentiometric, and iodometric method respectively.

The samples of stable oxygen and hydrogen isotopes were measured at the laboratory of Department of Geology at the University of Namibia using an off-axis integrated cavity output spectroscope (Los Gatos DLT-100). Measurements were normalized to Vienna Standard Mean Ocean Water (VSMOW).

All of these data were used to assess the groundwater quality by using single factor index method based on the guidelines of drinking-water quality of World Health Organization (WHO) and the guidelines of water of Namibia. In combination with the geology and hydrogeology, the dominant hydrogeochemical processes were analyzed in different locations in northwest Namibia by means of the conventional graphical and multivariate statistical methods.

4. Quality assessment of groundwater

Groundwater quality assessment, based on the guidelines for drinking water quality of the WHO and the guidelines of water in Namibia, was used to determine whether the groundwater was safe or acceptable for drinking purpose. It is helpful for the utilization, protection and management of groundwater. Some chemical contaminants, such as F^-, NO_3^-, NO_2^-, Mn, U and As, have been proven to cause severe health effects in humans as a consequence of prolonged exposure through drinking-water. F^-, NO_3^-, NO_2^-, Mn, U and As were used to assess the groundwater quality of the study area compared with the health-based guideline value of WHO (Table 1).

Although there is no health-based guideline value for turbidity, pH, TDS, total hardness, Cl^-, SO_4^{2-}, Na^+ and Fe in WHO guideline, the provision of drinking-water that is not only safe but also acceptable in appearance, taste and odor is of high priority. Because water that is aesthetically unacceptable will undermine the confidence of consumers, will lead to complaints and, more importantly, could lead to use of water from sources that are less safe (WHO, 2011). Reference is made to levels likely to cause complaints from consumers in WHO guideline. Turbidity, pH, TDS, total hardness, Cl^-, SO_4^{2-}, Na^+, Mn and Fe were used to assess the groundwater quality of the study area compared with the acceptability threshold of WHO guideline (Table 2). The pH of water usually has no direct impact on consumers, but it is one of the most important operational water quality parameters. According to the composition of the water and the nature of the construction materials used in the distribution system, it is usually in the range of 6.5–8.5. The turbidity, Mn and Fe at levels below 5 NTU, 0.3 mg/L and 0.1 mg/L are acceptable in appearance for most consumers, respectively. The TDS, total hardness, chloride, sulfate, and sodium at levels below 1000 mg/L, 500 mg/L, 250 mg/L, 250 mg/L, 200 mg/L are acceptable in taste for most consumers, respectively.

The guideline of water in Namibia was also applied to assess the groundwater quality in the area. This guideline divided the groundwater into four types. A: excellent quality water; B: good quality water; C: low risk water; D: high risk or water unsuitable for human consumption.

It should be noticed that the groundwater quality assessment in this study mainly deals with the inorganic compositions, while it does not include organic compositions and bacteria etc. Thus the suitability of groundwater for drinking was assessed from the viewpoint of inorganic compositions of concerns only.

Table 1
Drinking-water quality standard of World Health Organization—health-based targets.

Indicators	F^- mg/L	NO_3^- (as N) mg/L	NO_2^- (as N) mg/L	Mn mg/L	U mg/L	As mg/L
Health criterion	1.5	11	0.9	0.4	0.03	0.01

4.1. Assessment based on health-based targets

The assessment results based on health-based targets are listed in Table 3 with the excess values highlighted, showing that most of the groundwater samples are safe for human consumption in the area. However, the concentration of As, U and F^- in sample WOV are 9 times, 2 times and 2.6 times higher than that of the health standard, respectively. The concentration of fluoride in samples NW4, NW4H, AT3 and AT4 are 1.5–2 times higher than that of the standard. The nitrate concentration in samples NW9 and NW15 reached the health-based targets. And, NW11 has also been visibly polluted by animal wastes. Therefore, these waters cannot be used as drinking water, even though the chemical compositions meet the drinking water quality requirement.

4.2. Assessment based on acceptability threshold

According to the result of water quality single factor assessment based on acceptable threshold in Table 4, in which the excess values are highlighted in bold, most of the samples have one or more composition concentrations over the acceptable threshold. Only a few samples, NW10, NW11, NW8, NW3, and NW2, are acceptable in appearance and tastes. Most of the samples of Group B have high values in turbidity, total hardness and TDS. Samples of Group C have high values in total hardness and SO_4^{2-} concentration, and Group D and E have high values in TDS, Cl^- and Na^+ concentrations. These high values exceed the acceptable threshold and give the water bad appearance and tastes which could cause consumer dissatisfaction. Furthermore, a few samples in Group B and C have high Mn and Fe concentrations, which can cause undesirable tastes in beverages and strain sanitary ware and laundry. The acceptability thresholds, however, are not precise values, and tastes or appearance may be detectable by consumers at lower or higher levels, which depends on individual and local circumstances (WHO, 2011).

4.3. Assessment based on the guideline of water in Namibia

The assessment results based on the guideline of water in Namibia are showed in Table 5. According to the guideline of water in Namibia, water of Group A belongs to excellent quality water. NW6 and NW8 of Group B are of high risk or unsuitable for human consumption. In Group C and D, NW4 is unsuitable for human consumption, but the others are good quality or low health risk. Water of Group E is unfit for drinking, except for AT2 and AT5. According to the Langelier Index and Ryznar Index, almost all of the groundwater is scaling, and according to the Corrosivity ratio, most of the water has an increasing corrosive tendency. The Langelier Index (LI) is an approximate measure of the degree of saturation of calcium carbonate in water. It is calculated using the pH, alkalinity, calcium concentration, TDS, and water temperature.

Table 2
Drinking-water quality standard of World Health Organization—acceptability threshold.

Indicators	pH	Turbidity (NTU)	TDS mg/L	Total hardness mg/L	Cl^- mg/L	SO_4^{2-} mg/L	Na^+ mg/L	Mn mg/L	Fe mg/L
Acceptability threshold	6.5–8.5	5	1000	500	250	250	200	0.1	0.3

Table 3
Assessment result of single factor pollution index method based on health-based targets.

Sample ID		Health-based targets					
		1.5	11	0.9	0.4	0.03	0.01
		F^- (mg/L)	NO_3^- (as N) (mg/L)	NO_2^- (as N) (mg/L)	Mn (mg/L)	U (mg/L)	As (mg/L)
A	NW10	0.6	0.9	< 0.1	0.01	< 0.01	< 0.01
	NW11	0.9	< 0.5	< 0.1	< 0.01	< 0.01	< 0.01
B	NW6	0.2	4.7	< 0.1	0.24	< 0.01	< 0.01
	NW8	0.1	1.1	< 0.1	0.03	< 0.01	< 0.01
	NW9	0.2	**11**	< 0.1	0.01	< 0.01	< 0.01
	NW12	0.9	6.4	< 0.1	0.01	< 0.01	< 0.01
	NW13	0.8	< 0.5	< 0.1	0.05	< 0.01	< 0.01
	NW5	0.6	1.1	< 0.1	0.35	< 0.01	< 0.01
	NW5A	0.5	0.9	< 0.1	0.24	< 0.01	< 0.01
C	NW3	0.2	3.3	< 0.1	< 0.01	< 0.01	< 0.01
	NW4	**2.4**	< 0.5	< 0.1	0.01	< 0.01	< 0.01
	NW4H	**2.5**	< 0.5	< 0.1	< 0.01	< 0.01	< 0.01
	NW14B	0.8	5.7	< 0.1	< 0.01	< 0.01	< 0.01
	NW15	1.2	**11**	< 0.1	< 0.01	0.01	< 0.01
D	NW1	0.8	3	< 0.1	< 0.01	< 0.01	< 0.01
	NW2	0.4	1.3	< 0.1	< 0.01	< 0.01	< 0.01
E	AT1	1	0.5	< 0.1	0.2	< 0.01	< 0.01
	AT2	1	< 0.5	< 0.1	0.01	< 0.01	< 0.01
	AT3	**2.6**	< 0.5	< 0.1	< 0.01	0.01	0.01
	AT4	**3.1**	< 0.5	< 0.1	< 0.01	< 0.01	0.01
	AT5	1.2	< 0.5	< 0.1	< 0.01	< 0.01	< 0.01
	WOV	**3.9**	3.3	< 0.1	< 0.01	**0.06**	**0.09**

The values of each composition are actually measured value in this table. The excess values are highlighted in bold.

LI > 0 means the water is scaling, LI = 0 means the water is stable, and LI < 0 means the water is corrosive. The Ryznar Index (RI) has the same function as the saturation index of calcium carbonate, but is more accurate. It is used to assess the extent of water causing fouling or corrosion. RI < 6.5 means the water is scaling, RI > 7.5 means the water is corrosive, RI > 6.5 and < 7.5 means the water is stable. The Corrosivity ratio (CR) is used to evaluate the erosion ability of groundwater to concrete. CR < 0.2 means the water has no corrosive properties, CR > 0.2 means the water has increasing corrosive tendency.

5. Hydrogeochemical processes of groundwater

5.1. Stable hydrogen and oxygen isotope signature

The correlation between δD and $\delta^{18}O$ values of water samples from study area is displayed in Fig. 5. The samples plot near the Global Meteoric Water Line (GMWL). This indicates that the groundwater was recharged by precipitation. Overall there is a trend found that the samples from western and driest part of the study area show less depleted values than in the eastern, wetter part of the study area indicating an precipitation amount effect.

In Cuvelai-Etosal basin, groundwater samples of Group C, D and E show obvious differences in the values of δD and $\delta^{18}O$. This is likely to be caused by an altitude effect. Generally, the value of δD and $\delta^{18}O$ are gradually decreasing with an increasing of the recharge mountain elevation.

Table 4
Assessment of single factor pollution index method based on acceptability threshold.

Sample ID		Acceptability threshold								
		6.5–8.5	5	1000	500	250	250	200	0.1	0.3
		pH	Turbidity (NTU)	TDS (mg/L)	Total hardness (mg/L)	Cl^- (mg/L)	SO_4^{2-} (mg/L)	Na^+ (mg/L)	Mn (mg/L)	Fe (mg/L)
A	NW10	8.4	1.8	570	242	33	104	81	0.01	0.01
	NW11	8.0	0.50	815	492	73	146	107	< 0.01	0.02
B	NW6	7.3	1.7	543	448	7	30	6.8	**0.24**	< 0.01
	NW8	8.1	0.70	415	294	5	9.1	5.7	0.03	0.12
	NW9	8.0	**57**	**1131**	**817**	79	220	96	0.01	< 0.01
	NW12	8.2	0.80	**1149**	**817**	104	189	116	0.01	0.03
	NW13	8.2	**46**	734	**585**	28	41	52	0.05	0.15
	NW5	8.1	0.45	**1481**	**1278**	18	**847**	96	**0.35**	0.02
	NW5A	8.1	**178**	**1380**	**1295**	20	**978**	116	**0.24**	**10**
C	NW3	8.1	0.40	533	347	23	12	15	< 0.01	0.05
	NW4	8.1	**105**	827	**853**	123	**381**	33	0.01	**13**
	NW4H	8.0	1.3	848	**550**	22	**369**	33	< 0.01	0.07
	NW14B	7.9	0.25	605	**530**	22	31	20	< 0.01	< 0.01
	NW15	8.5	0.20	**1103**	**808**	91	**324**	86	< 0.01	0.02
D	NW1	7.5	0.15	**1487**	515	**311**	171	**299**	< 0.01	0.01
	NW2	8.4	0.85	645	362	84	42	70	< 0.01	0.01
E	AT1	8.0	**203**	**2057**	408	**559**	251	**527**	**0.20**	0.19
	AT2	7.8	0.15	**1796**	500	**426**	233	**423**	0.01	0.01
	AT3	8.5	2.2	**3162**	177	**879**	**432**	**1000**	< 0.01	0.04
	AT4	8.4	0.10	**2707**	196	**704**	**362**	**799**	< 0.01	0.03
	AT5	8.0	0.15	935	**525**	124	81	125	< 0.01	0.03
	WOV	**8.6**	3.3	**1501**	14	102	73	**588**	< 0.01	0.23

The values of each composition are actually measured value in this table. The excess values are highlighted in bold.

Table 5
Assessment result based on the guideline of water in Namibia.

Sample ID		Turbidity	EC	Total hardness	Cl^-	F^-	SO_4^{2-}	Na^+	Mg^{2+}	Fe	Langelier index	Ryznar index	Corrosivity ratio
A	NW10	B	A	A	A	A	A	A	A	B	SC	ST	ICT
	NW11	A	A	B	A	A	A	B	A	B	SC	SC	ICT
B	NW6	B	A	B	A	A	A	A	A	A	SC	ST	NCO
	NW8	A	A	A	A	A	A	A	A	B	SC	CO	NCO
	NW9	**D**	B	**C**	A	A	B	A	**C**	B	SC	SC	ICT
	NW12	A	B	**C**	A	A	A	B	**C**	B	SC	SC	ICT
	NW13	**D**	A	B	A	A	A	A	B	B	SC	SC	NCO
	NW5	A	B	**C**	A	A	**C**	A	**D**	A	SC	SC	ICT
	NW5A	**D**	B	**C**	A	A	**C**	B	**D**	**D**	SC	SC	ICT
C	NW3	A	A	B	A	A	A	A	B	A	SC	CO	NCO
	NW4	**D**	A	**C**	A	**C**	B	A	**C**	**D**	SC	SC	ICT
	NW4H	B	A	B	A	**C**	B	A	**C**	A	SC	ST	ICT
	NW14B	A	A	B	A	A	A	A	A	B	SC	SC	NCO
	NW15	A	B	**C**	A	A	B	A	**C**	B	SC	SC	ICT
D	NW1	A	B	B	B	A	A	B	A	A	SC	SC	ICT
	NW2	A	A	B	A	A	A	A	A	A	SC	SC	ICT
E	AT1	**D**	**C**	B	B	A	B	**C**	A	B	SC	SC	ICT
	AT2	A	B	B	B	A	B	**C**	A	B	SC	SC	ICT
	AT3	B	**D**	A	**C**	**C**	B	**D**	A	B	SC	ST	ICT
	AT4	A	**D**	A	**C**	**D**	B	**C**	A	B	SC	ST	ICT
	AT5	A	A	B	A	A	A	B	A	B	SC	SC	ICT
	WOV	B	B	A	A	**D**	A	**C**	A	B	SC	CO	ICT

The C and D types of water are highlighted in bold. SC represented 'scaling', ST represented 'stable', CO represented 'corrosive', NCO represented 'no corrosive', ICT represented 'Increasing corrosive tendency'.

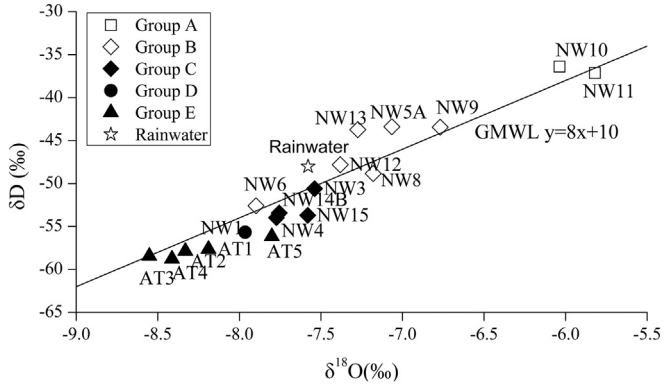

Fig. 5. δD vs. $\delta^{18}O$ of water samples in the study area.

5.2. Hydrochemical characteristics

5.2.1. Major ions

The values of TDS in Group A, B and C are < 1000 mg/L except for samples NW5, NW5A, NW9 and NW12 whose TDS is slightly higher than 1000 mg/L. The TDS of NW1 is higher than NW2. The reason may be that NW1 is closer to the Etosha Pan which is the discharge end of groundwater flow paths in Cuvelai-Etosal Basin. Except for AT5, the TDS of Group E is 2000–3000 mg/L which is the largest value in the study area. The TDS of sample AT5 is 930 mg/L.

The hydrochemical-types of the samples are shown in Table 6. Except for the samples NW5, NW5A, NW4 and NW4H, which are Mg-SO_4 type, the water types are Mg-HCO_3 for all other samples in Group A, B and C. In Group D, NW2 is Mg-HCO_3 type, and NW1 is Na-HCO_3 type. The latter has higher TDS and is located closer to the discharge zone. In Group E, AT5 is Mg-HCO_3 type with low TDS. WOV and AT2 are Na-HCO_3 types, while the others are Na-Cl types.

5.2.2. Trace and minor constituents

Concentrations of trace and minor constituents (Fe, Mn, F^-, U, As, NO_3^-, and NO_2^-) are presented in Table 3 and Table 4. Concentrations of Fe and Mn are higher in a few samples (NW5, NW5A, NW6, and NW4) of Group B and Group C, and AT1 of Group E, with the maximum of 13 mg/L and 0.35 mg/L respectively. The concentrations of Fe and Mn in the rest samples are < 0.05 and 0.023 mg/L respectively. Concentrations of F^- in AT3, AT4 and WOV of Group E and NW4 and NW4H of Group C are higher, and range from 2.4 to 3.9 mg/L. The concentrations of F^- in other samples are < 1.2 mg/L. Br^- is undetectable in the samples of Group C and some of Group A and B. The detectable Br^- concentrations in other samples are from 0.05 to 2.3 mg/L in the groundwater. Concentrations of U and As are higher in WOV, being 0.06 mg/L and 0.09 mg/L respectively. In AT3 and AT4 of group E, the U and As are detected to be 0.01 mg/L. The concentrations of U and As in other samples are below the detectable limit 0.01 mg/L. The nitrate concentrations in the study area are 0.5 to 11 mg/L (nitrate as N). Except for NW9 and NW15, the nitrate concentrations of the samples are less than the WHO limit of 11 mg/L. The nitrite concentrations are below the detectable limit 0.5 mg/L (nitrite as N) in the study area.

5.3. Hydrochemical processes

Based on the major cations (Na^+, Ca^{2+}, Mg^{2+}) and major anions (Cl^-, HCO_3^-, SO_4^{2-}) contents in the groundwater samples, the Piper diagram was plotted (Fig. 6), and different hydrochemical processes identified. Owing to low concentrations, K^+ and CO_3^{2-} were not considered in the Piper diagram in this study. Most of the contents of K^+ are < 5 mg/L, which is much lower than that of Na^+. Just a few samples contain CO_3^{2-}, with maximum of 9.6 mg/L.

The Mg-SO_4 type samples NW4H, NW4, NW5, NW5A, and NW15 differ from the surrounding Mg-HCO_3 type samples in Group A, B and C. This indicates the process of sulfate increasing. In Group D and E, the hydrochemical types change from Mg-HCO_3 type to Na-Cl type with increasing TDS, which indicates the salinization process.

The correlation between the compositions of the samples was calculated to study the relationship among different components. Table 7 presents the correlation coefficient of the physicochemical variables of groundwater. TDS correlates strongly with Na^+, Cl^-, alkalinity and Br^-. Alkalinity correlates fairly with Na^+ and TDS. Hardness correlates strongly with Ca^{2+}, Mg^{2+} and SO_4^{2-}. Cl^- correlates strongly with TDS, Na^+ and Br^-. F^- correlates fairly with Na^+. SO_4^{2-} correlates fairly with Mg^{2+}, Ca^{2+}, Mn and Fe. The turbidity correlates fairly with Fe. The mineralogy of a borehole located in Cuvelai-Etosal Basin shows

Table 6
Water types of the groundwater in the study area.

Group	Sample ID	TDS (mg/L)	Hydrochemical type	Group	Sample ID	TDS(mg/L)	Hydrochemical type
A	NW10	570	Mg·Na·HCO_3·SO_4	C	NW4H	848	Mg·SO_4·HCO_3
	NW11	815	Mg·Na·Ca·HCO_3·SO_4		NW15	1103	Mg·Ca·HCO_3·SO_4
B	NW6	543	Mg·Ca·HCO_3	D	NW2	645	Mg·Na·Ca·HCO_3·Cl
	NW8	415	Mg·HCO_3		NW1	1487	Na·Mg·Ca·HCO_3·Cl
	NW9	1131	Mg·Ca·Na·HCO_3·SO_4	E	AT5	935	Mg·Na·Ca·HCO_3·Cl
	NW12	1149	Mg·Na·HCO_3		WOV	1501	Na·HCO_3
	NW13	734	Mg·Ca·HCO_3		AT2	1796	Na·HCO_3·Cl
	NW5A	1380	Mg·Ca·SO_4·HCO_3		AT1	2057	Na·Cl·HCO_3
	NW5	1481	Mg·Ca·SO_4·HCO_3		AT4	2707	Na·Cl·HCO_3
C	NW3	533	Mg·HCO_3		AT3	3162	Na·Cl·HCO_3
	NW14B	605	Mg·Ca·HCO_3	Rainwater	R1	6	Na·HCO_3·Cl
	NW4	827	Mg·Ca·SO_4·HCO_3	Seawater	S1	34,773	Na·Cl

that the stratum contain calcite, calcrete, ferroan dolomite, halite, pyrite and other minerals (Miller et al., 2010). There are numerous deposits such as iron ore, copper ore, ferromanganese ore in the Kaokoveld region and the west of Cuvelai-Etosal Basin (Shi et al., 2013; Yang et al., 2017). And a mass of precipitated calcium carbonates result in alkaline surface environment in these regions (Li et al., 2013). The oxidation of S-bearing minerals produces ferrous sulfate and sulfuric acid, which subsequently react with carbonates, leading to the increase of Fe, SO_4^{2-}, Ca^{2+} and Mg^{2+} concentration in groundwater. Accordingly, the increase of TDS is mainly attributed to the halite and carbonate dissolution, bromide increases with the increase of halite dissolution, the increase of hardness is mainly caused by the oxidation of S-bearing minerals and the dissolution of calcium and magnesium carbonate, and the iron and manganese increases with the increase of sulfate. There is no correlation between nitrate and other ions, and nitrate may most likely originate from the human activities rather than from mineral dissolution. Wanke et al. (2014) indicated that the nitrate in the hand dug wells in the northwest Namibia originated from manure by the isotopic composition of nitrogen and oxygen in dissolved nitrate.

5.3.1. *Factor analysis of water samples in the area*

The factor analysis was used to identify main factors that affect the hydrochemical characteristics of groundwater (Zhuang and Li, 2014). The first four factors are selected to represent the dominant hydrochemical processes. The output of the factor analysis (Table 8) reveals that the first four eigenvalues together account for over 81% of the total variability of the hydrochemical processes. Factor1 is related to TDS, sodium, chloride, bromide and alkalinity; it characterizes the influence of halite and carbonate in the water and this factor explains 37.18% of the variability. Factor2 is related to hardness, sulfate, calcium, magnesium, iron, manganese and turbidity. It characterized the influence of iron, manganese and sulfated salts. It explains 26.22% of the variability.

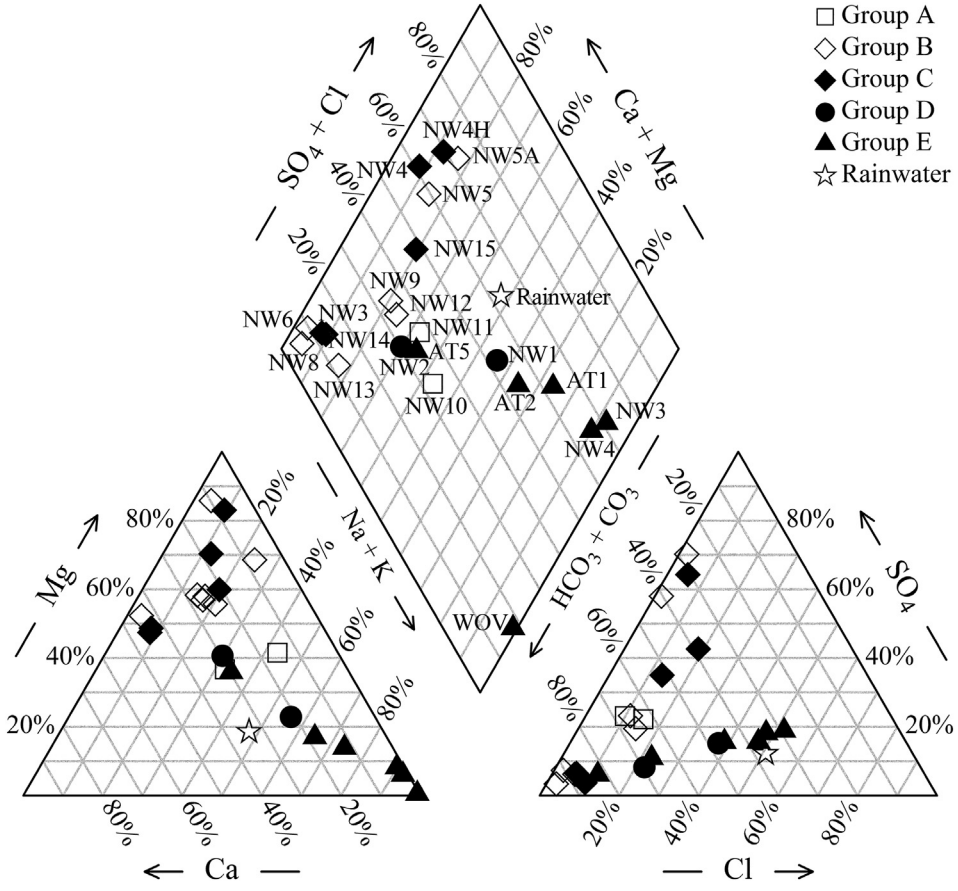

Fig. 6. Piper diagram of the water samples in the study area.

Table 7
Correlation coefficient of the physicochemical compositions of water samples.

	TDS	Alkalinity	Hardness	Cl^-	F^-	SO_4^{2-}	NO_3^-	Br^-	Na^+	Mg^{2+}	Ca^{2+}	Mn	Fe	Turbidity
TDS	1													
Alkalinity	**0.63**	1												
Hardness	− 0.14	− 0.15	1											
Cl^-	**0.92**	0.46	− 0.38	1										
F^-	0.54	0.46	− 0.37	0.46	1									
SO_4^{2-}	0.43	0.05	**0.7**	0.15	0.12	1								
NO_3^-	− 0.19	0.15	0.22	− 0.27	− 0.22	− 0.15	1							
Br^-	**0.7**	0.36	− 0.31	**0.75**	0.36	0.06	− 0.06	1						
Na^+	**0.94**	**0.66**	− 0.46	**0.92**	**0.65**	0.16	− 0.25	**0.7**	1					
Mg^{2+}	− 0.13	− 0.15	**0.95**	− 0.39	− 0.35	**0.68**	0.3	− 0.26	− 0.44	1				
Ca^{2+}	− 0.12	− 0.1	**0.81**	− 0.25	− 0.29	**0.55**	0.01	− 0.32	− 0.37	**0.59**	1			
Mn	0.08	0.01	0.54	− 0.12	− 0.3	**0.59**	− 0.14	0.04	− 0.1	0.48	**0.50**	1		
Fe	− 0.06	− 0.22	0.49	− 0.12	0.13	**0.5**	− 0.2	− 0.18	− 0.16	0.36	**0.58**	0.17	1	
Turbidity	0.16	− 0.01	0.38	0.11	− 0.07	0.43	− 0.15	− 0.05	0.04	0.28	0.44	0.43	**0.60**	1

The higher values are highlighted in bold.

Table 8
Vectors of loadings of factor analysis on the physicochemical compositions.

	Factor1	Factor2	Factor3	Factor4
TDS	**0.97**	0.136	− 0.061	0.063
Sodium	**0.95**	− 0.153	− 0.143	0.174
Chloride	**0.897**	− 0.113	− 0.229	0.062
Bromide	**0.794**	− 0.154	− 0.059	− 0.163
Total alkalinity	**0.706**	− 0.011	0.389	0.167
Total hardness	− 0.257	**0.893**	0.266	− 0.172
Sulfate	0.292	**0.864**	− 0.063	− 0.055
Calcium	− 0.239	**0.818**	− 0.001	− 0.044
Magnesium	− 0.229	**0.8**	0.369	− 0.215
Iron	− 0.189	**0.699**	− 0.333	0.489
Turbidity	0.068	**0.64**	− 0.37	0.065
Manganese	0.081	**0.619**	− 0.163	**− 0.615**
Nitrate	− 0.131	− 0.002	**0.883**	− 0.014
Fluoride	0.556	− 0.096	− 0.084	**0.683**

The higher loadings are highlighted in bold for each factor. The higher the loading coefficient, the higher the influence of that specie on the factor.

Factor3 is related to nitrate and characterizes the influence of animal wastes and anthropogenic pollution. This factor explains 10.62% of the variability. Factor4 is related positively to fluoride and negatively to manganese and explains just 7.39% of the variability.

The factor scores are given as linear combinations of the original standardized data with the factor loadings as the coefficients. The scores of the samples for the four factors are presented in Fig. 7. In Fig. 7a, the samples AT1, AT2, AT3, AT4, WOV and NW1 with higher scores for Factor1 characterize the influence of halite and carbonate. The samples NW5A, NW5 NW4, NW9, and NW15 with higher for Factor2 characterize the influence of iron, manganese and sulfated salts. The samples NW2, NW3, NW4H, NW6, NW8, NW10, NW11, NW13 and AT5 with lower scores for Factor1 and Factor2 are seldom affected by halite, carbonate, iron, manganese and sulfated salts. In addition, these samples have lower TDS as mentioned earlier. In Fig. 7b, the samples NW15, NW9, NW10, WOV and NW14B with higher scores for Factor3 characterize the influence of nitrate. The samples NW4, NW4H, and WOV with higher scores for Factor4 characterize the influence of fluoride. The other water samples in Fig. 7b are not affected by nitrate and fluoride.

5.3.2. *Salinisation mechanism analyses of groundwater*

In arid areas, mineral dissolution and evaporation are the main salinisation mechanisms for water bodies in inland plain areas (Huang and Pang, 2012). The Global Meteoric Water Line equation is given by $\delta D = 8\delta^{18}O + 10$ (Craig, 1961). The concept deuterium excess d is defined, for a slope of 8, as $d = \delta D\text{-}8\delta^{18}O$. d averages 10‰ for precipitation. When a water body undergoes evaporation, the deuterium excess will decrease and the salinity will increase. However, there is no obvious isotopic fractionation during plant transpiration or mineral dissolution (Huang and Pang, 2012). So we can use deuterium excess to determine the contributions of evaporation and mineral dissolution (or transpiration) to the salinity of groundwater in the study area.

Fig. 8, presenting the relationship between deuterium excess and TDS for the groundwater samples, shows that the deuterium excess values of groundwater in Group A and B are higher than 10‰ and in Group C, D and E lower than 10‰. The precipitation amount in Kaokoveld region is much lower than in Cuvelai-Etosal basin. This is consistent with deuterium excess having in general a negative correlation with the air humidity (Clark and Fritz, 1997). The TDS of groundwater samples of Group A、B and C show much less change than of Group E.

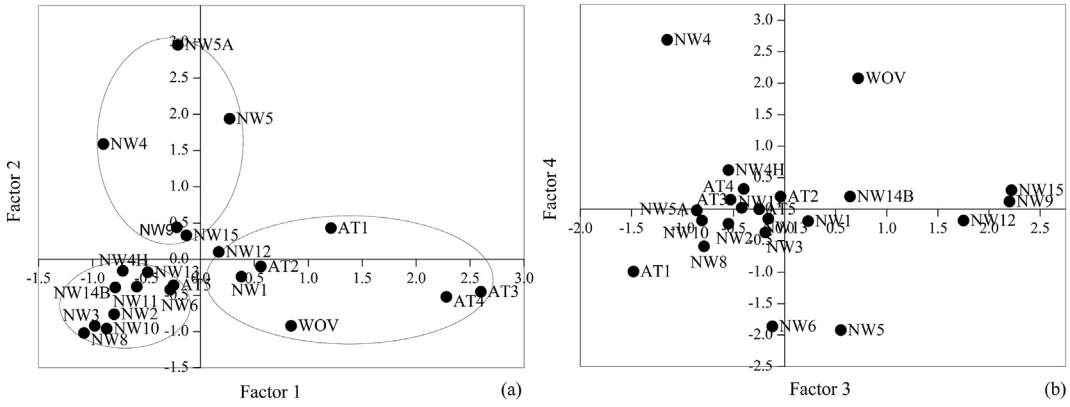

Fig. 7. Factor scores for water samples in the study area. (a) Factor1 vs. Factor2; (b) Factor3 vs. Factor4.

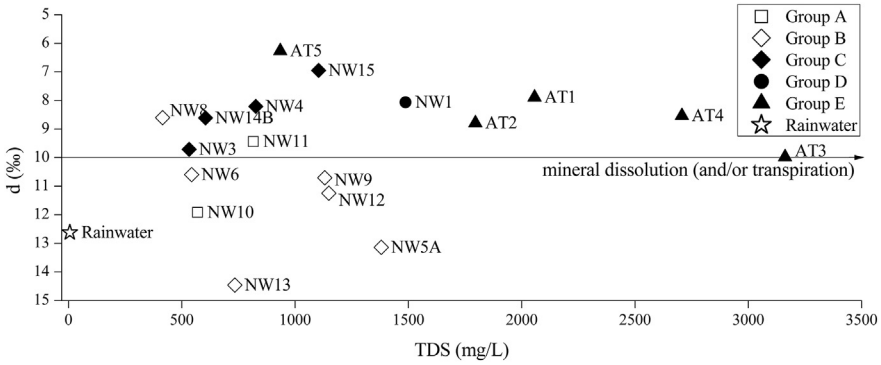

Fig. 8. Relationship between deuterium excess and TDS for groundwater in the study area.

However, the d values change only slightly with the great TDS increasing in Group E. This means that the increase in salinity of groundwater was not caused by evaporation but mineral dissolution mainly contributed to the salinity in the groundwater in Group E. According to the borehole samples (Miller et al., 2010) in the east of Etosha Pan, the sandy aquifers in the location of samples of Group D and E are confined, so the water of the samples of Group D and E didn't undergo the obvious evaporation process in the Etosha Pan but originates from the mineral dissolution. This is consistent with the result above.

5.3.3. Major ions and water-rock interactions

The scatter diagrams of groundwater chemistry components could reveal a clear variation in groundwater mineralization, mainly as a result of different mineral dissolutions. In order to distinguish the main water-rock interactions occurring in different locations of the study area, seven scatter diagrams were plotted (Fig. 9). If groundwater had undergone halite dissolution, the samples would have a good linear correlation in the plot of Na^+ vs. Cl^-. If samples are located on the line of y = x, all Cl^- and Na^+ of the samples originates from dissolution of halite. Fig. 9a shows that AT3, AT4, AT1, AT2, WOV and NW1 (of Group D and E) have undergone of halite dissolution, and that Na^+ has another sources except halite dissolution for most of the samples in the study area, such as cation exchange, which will be further discussed below.

The plot of Na^+ vs. ($Cl^- + SO_4^{2-}$) can be used to assess whether Na^+ combines with SO_4^{2-}. Fig. 9b shows that partial Na^+ of samples of AT3, AT4, AT1, AT2, WOV and NW1 (of Group D and E) have combined with SO_4^{2-}, but Na^+ in the samples has another sources as the $Na^+/(Cl^- + SO_4^{2-})$ is larger than 1. For samples of NW5A, NW5, NW4, NW4H, NW9, NW12, and NW15 (of Group B and C), the $Na^+/(Cl^- + SO_4^{2-})$ is much < 1, which may indicate that most of the SO_4^{2-} in the samples has another sources.

The plots of $Ca^{2+}+Mg^{2+}$ vs. HCO_3^- and ($Ca^{2+}+Mg^{2+}$) vs. ($HCO_3^- + SO_4^{2-}$) could reveal whether the Ca^{2+} and Mg^{2+} derived from the carbonate and sulfate dissolution. Fig. 9c and Fig. 9d show that all Ca^{2+}, Mg^{2+} and HCO_3^- of NW10, NW11,NW6,NW8,NW3, NW14B, NW2 and AT5 (of Group A, B, C, D and E) located on the line of y = x in the 9c, originate from carbonate dissolution; all Ca^{2+}, Mg^{2+}, HCO_3^- and SO_4^{2-} of all samples except AT3, AT4, AT1, AT2, WOV and NW1 (of Group D and E) derive from carbonate and sulfate dissolution (Fig. 9d). The samples AT3, AT4, AT1, AT2, WOV and NW1 have a higher concentrations of $HCO_3^- + SO_4^{2-}$ than that of $Ca^{2+} + Mg^{2+}$, indicating that either HCO_3^- or SO_4^{2-} have other sources and additional HCO_3^-, SO_4^{2-} might be combined with Na^+, or cation exchange occurred, which made $Ca^{2+}+Mg^{2+}$ decreased and Na^+ increased in the groundwater.

The plot of ($Ca^{2+}+Mg^{2+}$) vs. [$HCO_3^- + SO_4^{2-}$-(Na^+-Cl^-)] (Fig. 9e) shows that AT3, AT4, AT1, AT2, WOV and NW1 (of Group D and E) plot on the straight line of y = x. This confirms that they are likely to have undergone cation exchange. The plot of ($K^+ + Na^+$-Cl^-) vs. ($Ca^{2+} + Mg^{2+}$ –HCO_3^--SO_4^{2-}) (Fig. 9f) shows that samples, AT3, AT4, AT1, AT2, WOV and NW1 (of Group D and E), plot far away from the origin of coordinates indicating strong cation exchange. As dolomite and limestone are commonly available in Etosha Pan, it is likely that the dolomite and limestone dissolved in AT3, AT4, AT1, AT2, WOV and NW1 (of Group D and E), and produced much of calcium, magnesium, and bicarbonate. In addition, the existence of the pyrite and ferroan dolomite in the Cuvelai-Etosha Basin stratum (Miller et al., 2010) indicates the oxidation of pyrite in carbonate bearing stratum, which produced a certain amount of SO_4^{2-}, Ca^{2+} and Mg^{2+} (Shen, 1993), is likely to have happened. Owing to a great deal of halite existed in the stratum, the exchange between the calcium and magnesium in the groundwater and sodium in the stratum was easy to happen. This processes increased Na^+ concentration and additional Na^+ would combine with HCO_3^- and SO_4^{2-} (Fig. 9e).

5.3.4. Trace elements and water-rock interactions

Water constitutes can originate from natural or anthropogenic sources. The high nitrate concentrations were induced by inappropriate human activities in the study area. However, the trace elements in the study area mainly originate from natural sources such as rocks and sediments (Wanke et al., 2014).

Li et al. (2012) indicated that sedimentary iron ore had occurred in the Chous of Otavi Group in Kunene region. Fe may originate from minerals such as iron oxides or iron sulfides. The highest Fe concentrations occurred in NW4 and NW5A of Group B and C accompanying with the highest SO_4^{2-} concentrations (Fig. 10a). NW4H and NW5 with ORP of 89 and 199 mv respectively also have high SO_4^{2-} concentrations, but low Fe concentrations. The decrease of iron concentrations in NW4H and NW5 may be caused by the precipitation of iron hydroxides. Therefore, we infer that the Fe derives from the oxidation of pyrite. The chemical equations (Shen, 1993) of the oxidation of pyrite are as follows:

$$FeS_2 + 3.5O_2 + H_2O \rightarrow Fe^{2+} + 2SO_4^{2-} + 2H^+$$

$$Fe^{2+} + 6SO_4^{2-} + 3H_2O + 1.5O_2 \rightarrow 4Fe^{3+} + 6SO_4^{2-} + 2Fe(OH)_3$$

$$6Fe^{3+} + 9SO_4^{2-} + 18H_2O \rightarrow 6Fe(OH)_3 + 18H^+ + 9SO_4^{2-}$$

Owing to the existence of carbonate in the stratum, the free sulphuric acid which was produced in the reaction of pyrite oxidation would react with the carbonate.

$$H_2SO_4 + CaCO_3 \rightarrow Ca^{2+} + SO_4^{2-} + CO_2 + H_2O$$

or

$$H_2SO_4 + MgCO_3 \rightarrow Mg^{2+} + SO_4^{2-} + CO_2 + H_2O$$

These can account for the higher Fe, SO_4^{2-}, Ca^{2+} and Mg^{2+} concentration of NW4 and NW5A. The concentrations of Mn have relatively good correlation with SO_4^{2-}, Ca^{2+} and Mg^{2+}, which indicates that iron and manganese minerals may be concomitant.

The primarily conditions of formation of high fluorine groundwater

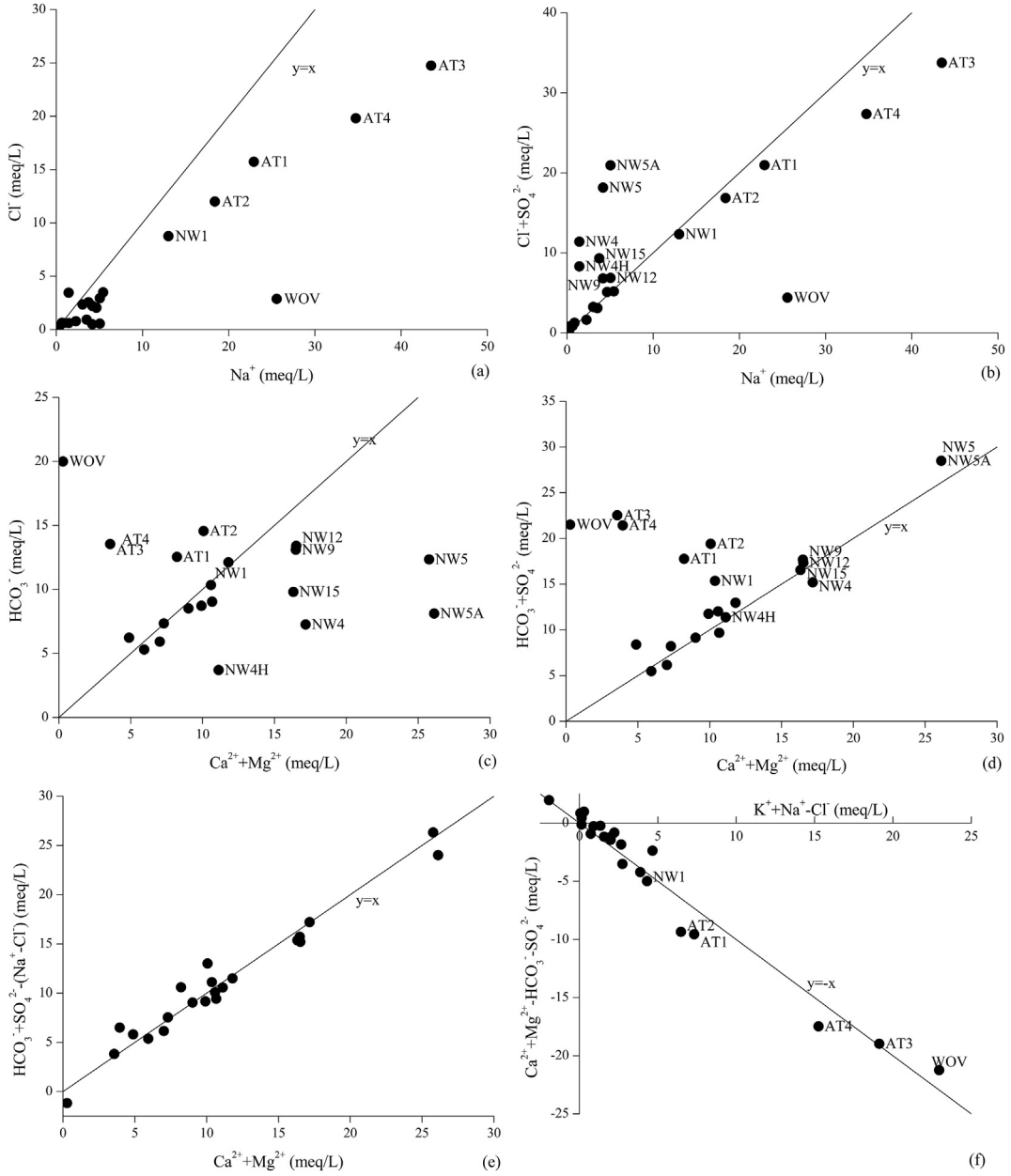

Fig. 9. Scatter plot of compositions of water samples in the study area. (a) Na^+ vs. Cl^-; (b) Na^+ vs. (Cl^- + SO_4^{2-}); (c) Ca^{2+} + Mg^{2+} vs. HCO_3^-; (d) (Ca^{2+} + Mg^{2+}) vs. (HCO_3^- + SO_4^{2-}); (e) (Ca^{2+} + Mg^{2+}) vs. [HCO_3^- + SO_4^{2-}-(Na^+-Cl^-)]; (f) (K^+ + Na^+-Cl^-) vs. (Ca^{2+} + Mg^{2+}-HCO_3^--SO_4^{2-}); (g) Fe vs. SO_4^{2-}.

are the rocks, sediments and soils that provide rich sources of F^- (Zhu et al., 2010). The sources of F^- seem to be fluorine containing minerals, such as fluorapatite, fluorite and phlogopite. The primary sources of fluoride cannot be determined with certainly, but the concentrations of F^- seem to be controlled by the precipitation of fluorite (Zeng and Liu, 1996; Sracek et al., 2015). Water with low Ca^{2+} concentrations, where equilibrium with respect to the mineral fluorite is not often reached, enhances the mobilization and enrichment of F^- (Wang and Chen, 2015; Sracek et al., 2015). Fig. 10b indicates that in a certain Ca^{2+} concentration, the F^- concentrations are higher in Cuvelai-Etosha Basin than in Kaokoveld region, and that except for NW4 the concentrations of F^- are higher when the Ca^{2+} concentrations are lower. These suggest that the F^- sources are abundant in the rocks and sediments of Cuvelai-Etosha Basin and the concentration of Ca^{2+} controls the concentration of F^-.

Br^- and Cl^- have similar physical properties. Their contents in groundwater usually increase with the TDS increase. Fig. 10c shows that Br^- concentrations increase with increasing Cl^- concentrations, especially in the samples of NW1, AT1, AT3, and AT4, which are located to the south and southeast of Etosha Pan, indicating Br^- and Cl^- originate from halite dissolution. This further confirms the groundwater in Group D and E have undergone minerals dissolution.

Arsenic presents in different minerals and solid phases of sediments. Sulfide minerals and iron oxides are the As rich minerals. And pyrites are the As richest sulfide minerals (Gao et al., 2014). The As in the sediments is strongly adsorbed on iron, manganese and aluminum oxide/hydroxides in oxic environment. This kind of As is easily leached out by alkaline bicarbonate water or released in the water after burial of the sediments when anoxic conditions develop (Anawar et al., 2003; Gao et al., 2014). The enrichment processes of As in groundwater are mainly three types: (1) oxidation of As rich sulfide (pyrite), (2) anion exchange (HCO_3^-, OH^-, NO_3^-, or PO_4^{3-} ions substitute As from the surface of minerals and sediments) and (3) reductive dissolution of iron, manganese and aluminum hydroxides in anoxic environment. Variant

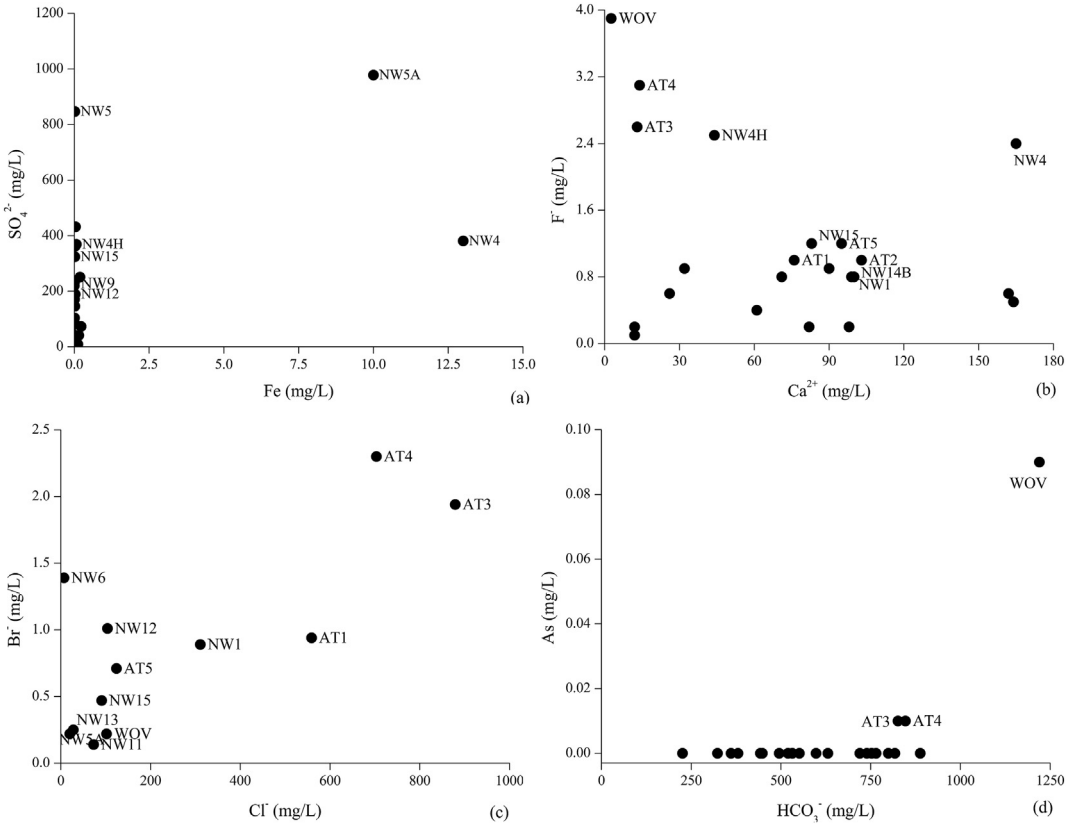

Fig. 10. Relationships of (a) Fe vs. SO_4^{2-}, (b) Ca^{2+} vs. F^-, (c) Cl^- vs. Br^-, and (d) HCO_3^- vs. As.

component contents (Fe, HCO_3^-, OH^-, NO_3^-, PO_4^{3-}, SO_4^{2-}, organic matter, et al.) in groundwater can indicate different enrichment processes of As. Water sample WOV has high As concentration with high HCO_3^- contents (Fig. 10d), low Fe and SO_4^{2-} contents, and the pH value of 8.6 (Table 2 and Table 3), indicating that the enrichment of As in WOV may result from the anion exchange. The high concentration HCO_3^- substitutes arsenic from the surface of sediments resulting in release of As to groundwater. The As is also detected in samples AT3 and AT4, demonstrating there are As rich sediments in the east of Cuvelai-Etosha Basin.

Weak alkaline environment and higher HCO_3^- contents are helpful to dissolve uranium-bearing minerals to form soluble U complex in water which can cause the increase of U concentration in groundwater (Yue and Wang, 2011; Du and Cheng, 2016). The higher U content in WOV seems to be related to the higher HCO_3^- content and higher pH value.

6. Conclusions

The water quality assessment shows that most of the water tested in the study area is safe to human consumption, but a majority of the samples are unacceptable in appearance and tastes. A few samples in Cuvelai-Etosha Basin had higher F^- concentrations. Fe and Mn contents were higher in some samples of Kaokoveld region. Nitrate concentrations in most of the samples did not exceed the WHO limit. The relatively higher nitrate contents were induced by inappropriate human activities.

The isotope data analysis indicates the groundwater in the study area was recharged by the precipitation. The salinity of the groundwater in the study area is mainly due to the minerals dissolution instead of evaporation. The major water-rock interaction processes are different in different places. Some samples located in Cuvelai-Etosha Basin and Kaokoveld region were low in TDS ($<$ 800 mg/L), and characterized by the influence of carbonate dissolution with dominant ions of HCO_3^- and Mg^{2+}. A part of the samples located in Kaokoveld region and the west of Cuvelai-Etosha basin with TDS of 800 mg/L to 1500 mg/L have experienced carbonate dissolution and pyrite oxidation. The dominant ions of them are SO_4^{2-} and Mg^{2+}. Most of the samples located to the east of Etosha Pan with TDS of 1500 mg/L to 3200 mg/L have undergone halite, carbonate dissolution and strong cation exchange with dominant ions of Na^+, Cl^- and HCO_3^-.

Water-rock interaction also dominated the concentrations and distribution of trace elements in groundwater. The higher Fe contents in some samples of Kaokoveld region can be explained by pyrite oxidization. The contents of F^- seem to be controlled by the Ca^{2+} concentrations in groundwater. Br^- concentrations increase with increasing Cl^- concentrations especially in the samples of Cuvelai-Etosha Basin, suggesting Br^- in groundwater was mainly from halite dissolution. High contents of As and U occurred in the groundwater in the east of Cuvelai-Etosha Basin. Weak alkaline environment and higher HCO_3^- concentrations seem to be responsible for the higher As and U concentrations in the groundwater. Knowledge of these associations could enhance the understanding of distributions and sources of major ions and trace elements in groundwater and could have implications for the management and utilization of groundwater resources in the region and other similar areas.

Acknowledgements

This work is supported by China-Africa Universities 20 plus 20 Cooperation Plan, National Natural Science Foundation of China (41672243, U1602233, 40930637, 41272269), Fundamental Research Funds for the Central Universities (2652015316). We thank Mr. Liu Dianbo, Ms. Zhang Sufen, Mr. Li Ming, Mr. Cao Hai, Mr. Henry Beukes, Dr. Ansgar Wanke and others for coordination and assistance in field work. We gratefully acknowledge comments and helpful information

from the Editors Dr. Robert Ayuso and Dr. Martin F Soto Jimenez and the anonymous reviewers.

References

Anawar, H.M., Akai, J., Komaki, K., Terao, H., Yoshioka, T., Ishizuka, T., Safiullah, S., Kato, K., 2003. Geochemical occurrence of arsenic in groundwater of Bangladesh: sources and mobilization processes. J. Geochem. Explor. 77 (2–3), 109–131. http://dx.doi.org/10.1016/S0375-6742(02)00273-X.

Bao, R.X., Hao, F.L., Liu, D.T., Shi, S.P., 1998. Water resources in Namibia and study of water supply in central northern Namibia. Design Water Resour. Hydroelec. Eng. 3, 41–43 (in chinese).

Christelis, G., Struckmeier, W., 2001. Groundwater in Namibia—An Explanation to the Hydrogeological Map.

Chukwura, U.O., Udom, G.J., Cuthbertetal, S.J., 2015. Evaluation of hydrochemical characteristics and flow directions of groundwater quality in Udi Local Government Area Enugu State, Nigeria. Environ. Earth Sci. 73, 4521–4555. http://dx.doi.org/10.1007/s12665-014-3741-4.

Clark, I., Fritz, P., 1997. Environmental Isotopes in Hydrology. CRC press/Lewis Publishers, Boca Raton.

Craig, H., 1961. Isotopic variations in meteoric waters. Science 133, 1702–1703. http://dx.doi.org/10.1126/science.133.3465.1702.

Du, J.M., Cheng, L., 2016. Investigation for total radioactivity abnormal ratio in underground water of Jinzhong city of Shanxi province. Radiat. Prot. 36 (4), 249–251 259. (in Chinese).

Feng, S.Z., Zhang, Z.S., 2012. Quality evaluation of lake water and sediment based on multilevel fuzzy theory. Meteoro. Environ. Res. 3 (8), 24–27 (35).

Gao, C.R., Feng, C.E., Liu, W.B., Akai, J., Kuboda, Y., Kobayashi, I., 2014. Patterns of arsenic cycle and groundwater arsenic contamination on the earth's surface. Acta Geosci. Sin. 35 (6), 741–750. http://dx.doi.org/10.3975/cagsb.2014.06.10.

Gibbs, R.J., 1970. Mechanisms controlling world water chemistry. Science 170 (3962), 1088–1090. http://dx.doi.org/10.1126/science.170.3962.1088.

Güler, G., Thyne, G.D., Mccray, J.E., Turner, K.A., 2002. Evaluation of graphical and multivariate statistical methods for classification of water chemistry data. Hydrogeol. J. 10, 455–474. http://dx.doi.org/10.1007/s10040-002-0196-6.

Huang, T.M., Pang, Z.H., 2012. The role of deuterium excess in determining the water salinisation mechanism: a case study of the arid Tarim River Basin, NW China. Appl. Geochem. 27 (12), 2382–2388. http://dx.doi.org/10.1016/j.apgeochem.2012.08.01 5.

Kluge, T., Liehr, S., Lux, A., Moser, P., Niemann, S., Umlauf, N., Urban, W., 2008. IWRM concept for the Cuvelai Basin in northern Namibia. Phys. Chem. Earth 33, 48–55. http://dx.doi.org/10.1016/j.pce.2007.04.005.

Li, Q., Li, M., Zhao, M.W., Wang, W.Q., Shi, C.Q., Kong, C., Luan, J., 2012. Geological characteristics and development prospects of sedimentary metamorphic iron deposit of Upper Proterozoic Age in northwestern Namibia. Miner. Explor. 3 (6), 845–849 (in Chinese).

Li, Q., Li, M., Xi, X.F., Zhang, D.F., Shi, C.Q., Wang, W.Q., 2013. A study on the genesis of the copper enrichment in earth surface in Namibia and significance [J]. Mineral Explor. 4 (01), 92–96 (in Chinese).

Lindenmaier, F., Miller, R., Fenner, J., Christelis, G., Dill, H.G., Himmelsbach, T., Kaufhold, S., Lohe, C., Quinger, M., Schildknecht, F., Symons, G., Walzer, A., Wyk, B.V., 2014. Structure and genesis of the Cubango Megafan in northern Namibia: implications for its hydrogeology. Hydrogeol. J. 22, 1307–1328. http://dx.doi.org/10.1007/s10040-014-1141-1.

Miller, R.M., Pickford, M., Senut, B., 2010. The geology palaeontology and evolution of the Etosha Pan, Namibia: implications for terminal Kalahari deposition. S. Afr. J. Geol. 113 (3), 307–334. http://dx.doi.org/10.2113/gssajg.113.3.307.

Qian, H., Li, P.Y., Wu, J.H., Zhou, Y.H., 2013. Isotopic characteristics of precipitation, surface and ground waters in the Yinchuan plain, Northwest China. Environ. Earth Sci. 70, 57–70. http://dx.doi.org/10.1007/s12665-012-2103-3.

Qian, H., Wu, J.H., Zhou, Y.H., Li, P.Y., 2014. Stable oxygen and hydrogen isotopes as indicators of lake water recharge and evaporation in the lakes of the Yinchuan plain. Hydrol. Process. 28, 3554–3562. http://dx.doi.org/10.1002/hyp.9915.

Schwartz, M.O., 2006. Numerical modelling of groundwater vulnerability: the example Namibia. Environ. Geol. 50 (2), 237–249. http://dx.doi.org/10.1007/s00254-006-0204-6.

Shan, M.L., Jin, M., Huo, M.Y., Zhang, D., Gao, Y., 2012. Ore-prospecting practice and understanding in east Kaoko belt of northwestern Namibia. J. Hunan Univ. Arts Sci. (Nat. Sci. Edit.) 24 (3), 18–21. (in Chinese). https://doi.org/10.3969/j.issn.1672-6146.2012.03.006.

Shen, Z.L., 1993. The Basis of Hydrogeochemistry. Geological Publishing House, Beijing, China.

Shi, J., Zhou, J., Lv, G.H., Zhang, J., 2013. Structure characteristics and deposit types in Northwest Namibia [J]. World Nonferr. Metal. 03, 66–69 (in Chinese).

Sracek, O., Wanke, H., Ndakunda, N.N., Mihaljevič, M., Buzek, F., 2015. Geochemistry and fluoride levels of geothermal springs in Namibia. J. Geochem. Explor. 148, 96–104. http://dx.doi.org/10.1016/j.gexplo.2014.08.012.

Wang, G.C., 1990. Equilibrium calculation of water-rock system: methods and cases. Hydroge. Eng. Geol. 20 (1), 41–43. (in Chinese). 10.16030/j.cnki.issn.1000-3665.1990.01.020.

Wang, Y.S., Chen, X.X., 2015. Spatial variation and genesis of groundwater fluoride in confined aquifer from the upper Qingshui river basin. J. Arid Land Resour. Environ. 29 (12), 170–176. (in Chinese). 10.13448/j.cnki.jalre.2015.419.

Wang, L.F., Hu, F.S., Yin, L.H., Wan, L., Yu, Q.S., 2013. Hydrochemical and isotopic study of groundwater in the Yinchuan plain, China. Environ. Earth Sci. 69, 2037–2057. http://dx.doi.org/10.1007/s12665-012-2040-1.

Wanke, H., Nakwafila, A., Hamutoko, J.T., Lohe, C., Neumbo, F., Petrus, I., David, A., Beukes, H., Masule, N., Quinger, M., 2014. Hand dug wells in Namibia: an underestimated water source or a threat to human health? Phys. Chem. Earth 76–78, 104–113. http://dx.doi.org/10.1016/j.pce.2015.01.004.

WHO, 2011. Guidelines for Drinking Water Quality. 1 World Health Organization (WHO), Geneva. http://www.who.int/water_sanitation_health/publications/2011/9789241548151_ch08.pdf?ua=1.

Yan, W.J., Liu, X.H., Zhu, W.B., Zhang, H., Zhang, Y., Li, F., Gao, Y., Lin, J.M., Zhang, W., 2015. An interpretation of magnetic anomalies of the buried faults in north Namibia. J. Geol. 39 (3), 456–461. (in Chinese). https://doi.org/10.3969/j.issn.1674-3636.2015.03.456.

Yang, Z.Y., Yang, H.B., 2015. Water quality assessment and cause analysis of typical lakes and reservoirs in the Fu River Basin. Heilongjiang Sci. Technol. Water Conserv. 43 (1), 201–203. (in Chinese). 10.07-7596(2015)01-0201-03.

Yang, S.S., Ruan, J., Zhou, X.J., Cen, M., 2017. On iron deposit genesis and potential area selection in Chuos formation in northwestern Namibia [J]. J. Geol. 41 (01), 124–128. (in Chinese). https://doi.org/10.3969/j.issn.1674-3636.2017.01.124.

Yidana, S.M., Yidana, A., 2010. Assessing water quality using water quality index and multivariate analysis. Environ. Earth Sci. 59 (7), 1461–1473. http://dx.doi.org/10.1007/s12665-009-0132-3.

Yidana, S.M., Yakubo, B.B., Akabzaa, T.M., 2010. Analysis of groundwater quality using multivariate and spatial analyses in the Keta basin, Ghana. J. Afr. Earth Sci. 58, 220–234. http://dx.doi.org/10.1016/j.jafrearsci.2010.03.003.

Yue, S.J., Wang, G.C., 2011. Relationship between the hydrogeochemical environment and sandstone-type uranium mineralization in the Ili basin, China. Appl. Geochem. 26 (1), 133–139. http://dx.doi.org/10.1016/j.apgeochem.2010.11.010.

Zeng, J.H., Liu, W.S., 1996. A quantitative study on fluoride dissolution and precipitation in shallow groundwaters [J]. Earth Sci. (J. China U. Geosci.) 21 (3), 337–340 (in Chinese).

Zhang, X.Y., Zhang, Y.X., Ren, Z.Y., Duan, Z.L., 2014. Comparison and practical example of assessment method in different groundwater qualities. J. Water Resour. Water Eng. 25 (2), 98–101. in Chinese. 10.11705/j.issn.1672-643X.2014.02.20.

Zhu, Y., Yang, B.C., Zhao, A.N., et al., 2010. The formation regularity of high-fluorine groundwater in Dali County, Shaanxi Province. Geol. C. 37 (3), 672–675 (in Chinese).

Zhuang, Y., Li, Y.M., 2014. Evaluation of water source quality based on main component analytical method. Water Technol. 8 (4), 12–14. (in Chinese). https://doi.org/10.3969/j.issn.1673-9353.2014.04.004.